



Title	Pathogenic Roles of Cardiac Fibroblasts in Pediatric Dilated Cardiomyopathy
Author(s)	Tsuru, Hirofumi; Yoshihara, Chika; Suginobe, Hidehiro et al.
Citation	Journal of the American Heart Association. 2023, 12(13), p. e029676
Version Type	VoR
URL	https://hdl.handle.net/11094/92522
rights	This article is licensed under a Creative Commons Attribution-NonCommercial-NoDerivatives 4.0 International License.
Note	









The University of Osaka Institutional Knowledge Archive : OUKA

<https://ir.library.osaka-u.ac.jp/>

The University of Osaka

ORIGINAL RESEARCH

Pathogenic Roles of Cardiac Fibroblasts in Pediatric Dilated Cardiomyopathy

Hirofumi Tsuru , MD, PhD*; Chika Yoshihara, MD*; Hidehiro Sugimoto , MD*; Mizuki Matsumoto, MSc; Yoichiro Ishii, MD, PhD; Jun Narita , MD; Ryo Ishii, MD; Renjie Wang , MD; Atsuko Ueyama , MD; Kazutoshi Ueda, MD; Masaki Hirose , MD; Kazuhisa Hashimoto , MD; Hiroki Nagano, MD; Ryosuke Tanaka, MSc; Takaharu Okajima, PhD; Keiichi Ozono, MD, PhD; Hidekazu Ishida , MD, PhD

BACKGROUND: Dilated cardiomyopathy (DCM) is a major cause of heart failure in children. Despite intensive genetic analyses, pathogenic gene variants have not been identified in most patients with DCM, which suggests that cardiomyocytes are not solely responsible for DCM. Cardiac fibroblasts (CFs) are the most abundant cell type in the heart. They have several roles in maintaining cardiac function; however, the pathological role of CFs in DCM remains unknown.

METHODS AND RESULTS: Four primary cultured CF cell lines were established from pediatric patients with DCM and compared with 3 CF lines from healthy controls. There were no significant differences in cellular proliferation, adhesion, migration, apoptosis, or myofibroblast activation between DCM CFs compared with healthy CFs. Atomic force microscopy revealed that cellular stiffness, fluidity, and viscosity were not significantly changed in DCM CFs. However, when DCM CFs were cocultured with healthy cardiomyocytes, they deteriorated the contractile and diastolic functions of cardiomyocytes. RNA sequencing revealed markedly different comprehensive gene expression profiles in DCM CFs compared with healthy CFs. Several humoral factors and the extracellular matrix were significantly upregulated or downregulated in DCM CFs. The pathway analysis revealed that extracellular matrix receptor interactions, focal adhesion signaling, Hippo signaling, and transforming growth factor- β signaling pathways were significantly affected in DCM CFs. In contrast, single-cell RNA sequencing revealed that there was no specific subpopulation in the DCM CFs that contributed to the alterations in gene expression.

CONCLUSIONS: Although cellular physiological behavior was not altered in DCM CFs, they deteriorated the contractile and diastolic functions of healthy cardiomyocytes through humoral factors and direct cell–cell contact.

Key Words: cardiac fibroblast ■ cardiomyocyte ■ dilated cardiomyopathy ■ pediatric ■ RNA-seq

Pediatric cardiomyopathies are rare diseases, with an annual incidence of approximately 1 in 100 000 children. Dilated cardiomyopathy (DCM) is the most common phenotype, which is characterized by impaired systolic function and dilatation of the left ventricle, resulting in congestion and low cardiac output.^{1,2} DCM treatment involves drugs, including β -blockers, angiotensin-converting enzyme inhibitors, and diuretics, which target neurohormonal derangements. However,

patients who are refractory to these medications should receive left ventricular assist device implantation and heart transplantation.¹

Various causes of DCM have been investigated to date.² Recently, whole exome sequence and targeted next-generation sequencing studies have revealed causative gene variants, which primarily encode cardiomyocyte contractile components such as the sarcomere and sarcoplasmic reticulum.^{3–5} Heterozygous

Correspondence to: Hidekazu Ishida, MD, PhD, Department of Pediatrics, Osaka University Graduate School of Medicine, 2-2 Yamadaoka, Suita, Osaka 565-0871, Japan. Email: hideishi@ped.med.osaka-u.ac.jp

*H. Tsuru, C. Yoshihara, and H. Sugimoto contributed equally.

This article was sent to Julie K. Freed, MD, PhD, Associate Editor, for review by expert referees, editorial decision, and final disposition.

Supplemental Material is available at <https://www.ahajournals.org/doi/suppl/10.1161/JAHA.123.029676>

For Sources of Funding and Disclosures, see page 13.

© 2023 The Authors. Published on behalf of the American Heart Association, Inc., by Wiley. This is an open access article under the terms of the [Creative Commons Attribution-NonCommercial-NoDerivs](#) License, which permits use and distribution in any medium, provided the original work is properly cited, the use is non-commercial and no modifications or adaptations are made.

JAHA is available at: www.ahajournals.org/journal/jaha

RESEARCH PERSPECTIVE

What Is New?

- Cardiac fibroblasts (CFs) generated from patients with dilated cardiomyopathy exhibit distinctive gene expression patterns compared with healthy CFs, despite the fact that their physiological functions are not significantly altered.
- Dilated cardiomyopathy CFs may impair the systolic and diastolic function of healthy cardiomyocytes through humoral substances, extracellular matrix, and direct cell–cell interaction.

What Question Should be Addressed Next?

- It is necessary to elucidate which specific signaling molecules are associated with the pathogenicity of dilated cardiomyopathy CFs in order to develop a novel therapeutic strategy for dilated cardiomyopathy by modulating CF behaviors.

Nonstandard Abbreviations and Acronyms

CF	cardiac fibroblast
DCM	dilated cardiomyopathy
ECM	extracellular matrix
HCF	healthy cardiac fibroblast
RCM	restrictive cardiomyopathy
TGF	transforming growth factor

missense variants of *MYH7*, *MYBPC3*, *TTNC1*, *TNNT2*, *TNNI3*, *TPM1*, and *ACTC1* have been identified as sarcomere gene mutations, and those of *LAMP2*, *DES*, *SCN5A*, *FHOD3*, *BAG3*, and *MYPN* have been considered nonsarcomere gene mutations.^{1,6} However, it is noteworthy that different variants frequently cause similar cardiac phenotypes, whereas the same missense variants occasionally cause different cardiomyopathy phenotypes.^{7,8} In addition, pathologic gene variants are found in <50% of DCM cases despite thorough comprehensive gene analyses.^{1,9} Therefore, the relationship between genotype and phenotype may be limited in DCM, suggesting that entire DCM causes cannot be explained by genetic background and cellular abnormalities in cardiomyocytes.

Cardiomyocytes are not the only cell population associated with the heart. The heart is also composed of endothelial cells, smooth muscle cells, and cardiac fibroblasts (CFs). Of these, CFs account for 60% of the cells in the heart.^{10,11} Recently, several studies demonstrated that CFs can affect cardiomyocyte behavior in response to chemical, electrical, and mechanical

stimuli, suggesting that they play an important role in maintaining cardiac function under healthy conditions as well as during diseased states.^{12–14} Several studies have indicated that CFs interact with cardiomyocytes through humoral factors or the extracellular matrix (ECM), which functions as a scaffold for cardiomyocytes.^{15,16} Animal models mimicking myocardial infarction or hypertensive cardiac diseases have revealed that CFs play various roles in the damaged heart^{16–18}; however, their specific function in cardiomyopathy remains unclear. We recently demonstrated that CFs from idiopathic restrictive cardiomyopathy (RCM) patients impair the diastolic function of healthy cardiomyocytes.^{19,20} Therefore, we analyzed the cellular physiology and pathogenic roles of CFs derived from pediatric patients with DCM.

METHODS

Transparency and Openness Promotion Guidelines Statement

The data that support the findings of this study are available from the corresponding author upon reasonable request.

Institutional Review Board Approval

This project was approved by the Osaka University Clinical Research Review Committee (numbers 15211 and 442). The study conformed to the principles outlined in the Declaration of Helsinki. All animal procedures were performed in accordance with institutional guidelines. We obtained written informed consent from the parents of all of the minors included in this study.

Clinical Data Collection

Clinical characteristics and data for the patients were retrospectively collected from clinical records, including sex, age at diagnosis, age at sampling, medications at sampling, and serum B-type natriuretic peptide levels. The fibrosis ratio of left ventricle specimens from each patient was calculated using ImageJ software (<https://imagej.nih.gov/ij/>) following Masson trichrome staining of heart tissue sections. Five different locations were evaluated.

Cell Culture

CFs were cultured from tissues obtained from the left ventricular free wall at the time of heart transplantation as previously described.¹⁹ Briefly, cardiac specimens were minced, seeded onto cell culture dishes, and incubated in DMEM with 10% FBS and 1% penicillin/streptomycin. The majority of adherent cells were considered CFs as assessed by morphological

observation under an inverted phase contrast microscope and by immunocytochemistry using antibodies against von Willbrand factor and smooth muscle myosin heavy chain, as previously described.¹⁹ Cell culture was performed in a humidified incubator with a media change every 2 to 3 days. Three young healthy CF lines (13-year-old boy, 25-year-old women, and 30-year-old women; all White) were purchased from PromoCell and cultured the same way as the DCM CFs. Cells between passage numbers 4 and 7 were used for all experiments.

Proliferation Assay

Cells were seeded at 5×10^3 per well in a 96-well plate and incubated with DMEM and 10% FBS overnight. Then, $10 \mu\text{M}$ EdU was added and incubated for 24 hours. The percentage of EdU-positive nuclei was analyzed using an IN Cell Analyzer 6000 with Click-iT EdU Imaging Kit (ThermoFisher Scientific, Waltham, MA) according to the manufacturer's instructions. Three independent experiments were conducted for each assay.

Apoptosis and Myofibroblast Assay

The ratio of apoptotic cells and myofibroblasts were assessed as previously described.¹⁹ Briefly, cells were incubated for 48 hours under the following 4 conditions: (1) DMEM with FBS in a normoxic environment, (2) serum-free DMEM in a normoxic environment, (3) DMEM with FBS in a hypoxic environment (1% O_2), and (4) serum-free DMEM in a hypoxic environment (1% O_2). The percentage of caspase-3-positive apoptotic cells and cytoplasmic α -smooth muscle actin-positive myofibroblasts were counted with an IN Cell Analyzer 6000. Three independent experiments were conducted for each assay.

Migration Assay

Cells (3.0×10^4) were seeded into each well of a 96-well plate for 24 hours before assay. After confirming cell confluence, a scratch and vertical wound was introduced through the cell monolayer using a $10 \mu\text{L}$ pipette tip. The distance from 1 side of the wound to the other was measured, and the rate of shortening at 12 hours was analyzed using ImageJ software.

Attachment Assay

Cells (5.0×10^3) were seeded into each well of a 96-well plate. Nuclei were stained with Hoechst 33342, 4 hours after seeding (1:1000; Dojindo Molecular Technologies, Kumamoto, Japan), and the number of attached cells was counted with an IN Cell Analyzer (sum of cells at 20 fields per well).

Primary Culture of Healthy Rat Cardiomyocytes

Two-day-old Sprague-Dawley rats were used in accordance with the facility ethics committee's consent of Osaka University (number 01-043-001). Cardiomyocytes were obtained by modifying a previously published technique.^{19,21} The ventricular tissues were isolated and minced; thereafter, the tissue fragments were processed with trypsin and collagenase for 2 minutes in a 37°C water bath and filtered. After repeating this procedure 7 to 8 times, the cells were plated on cell culture plates in DMEM supplemented with 10% FBS and 1% penicillin/streptomycin. The nonadherent cells were collected 1 hour after incubation using the preplating procedure to eliminate non-myocytes for cardiomyocyte purification.²² Cells were maintained until coculture experiments were done in DMEM medium supplemented with 10% FBS.

Coculture of CFs With Cardiomyocytes

For direct 2-dimensional coculture experiments, CFs were seeded at 3.0×10^4 cells per well in a 96-well plate coated with 1% gelatin 24 hours before the initiation of coculture. After confirming full confluence of the CFs, healthy rat cardiomyocytes were seeded at 6.0×10^4 cells per well. For indirect coculture experiments, we used a $0.4 \mu\text{m}$ Transwell 96-well plate (Corning, Corning, NY) to evaluate the effect of humoral factors. CFs were seeded at 1.5×10^4 cells on an insert plate for 24 hours to obtain full confluence before coculture. Healthy rat cardiomyocytes were seeded at 6.0×10^4 cells on a 96-well plate coated with 1% gelatin, then cocultured with CFs in the upper chamber.²³ After 48 hours of coculture, we analyzed the function of the rat cardiomyocytes by assessing cellular motion and mRNA expression.

Motion Analysis of Cardiomyocytes

To evaluate both the contractile and diastolic function of cocultured cardiomyocytes, we used motion vector analysis with an SI8000 Cell Motion Imaging System (Sony, Tokyo, Japan). The cellular motion at each detection point was converted into a motion vector, and the motion velocity within each region of interest was calculated based on the sum of the vector magnitudes. For this analysis, the maximum contraction velocity corresponds to the contractile function of the cardiomyocytes, and the maximum relaxation velocity corresponds to the diastolic function. Movie images of spontaneous beating cardiomyocytes were captured as sequential phase-contrast images, with a $\times 10$ objective at a frame rate of 150 frames per seconds, a resolution of 2048×2048 pixels, and a depth of 8 bits.

Regions of interest were set to surround the cardiomyocyte nuclei and analyzed for contraction velocities, relaxation velocities, and beating rates.^{19,24} Data from isolated cardiomyocytes were used for the analysis. In indirect cocultures, 10 to 20 cells were counted in each patient in 1 experiment. In direct coculture, 30 to 40 cells were counted in each patient in 1 experiment. Three independent coculture experiments were performed in each cardiac fibroblast line from each patient.

Quantitative Polymerase Chain Reaction

After a 48-hour incubation period, cells from the direct and indirect coculture were harvested, and total RNA was extracted using a NucleoSpin RNA column kit (Takara Bio, Kusatsu, Japan). Reverse transcription and real-time polymerase chain reaction analyses were done using a Light-Cycler 480 with a Thunderbird SYBR quantitative polymerase chain reaction mix kit (Toyobo, Osaka, Japan) as previously described.¹⁹ The forward and reverse primer sets are presented in Table S1. Data were analyzed using the standard curve method. The cycle threshold was calculated using the default settings of the real-time sequence detection software (ThermoFisher Scientific). Three independent experiments were conducted in each CF line.

Whole Exome Sequencing

Whole exome sequencing was done to identify possible pathogenic variants for all patients with DCM and their parents as previously described.¹⁹ Prepared genomic libraries were sequenced on a HiSeq 3000 system (Illumina, San Diego, CA). The type of variant and its position on the gene were determined from the annotation of University of California Santa Cruz Known Genes, RefSeq genes, and Ensemble genes. Candidate variants were evaluated for 257 genes associated with cardiomyopathy, and those with a minor allele frequency <0.5% were extracted. To determine the potential functional effects of the variants, 4 bioinformatic algorithms were used: Human Gene Mutation Database, InterVar, Combined Annotation Dependent Depletion (CADD), and protein variation effect analyzer. Missense variants were considered pathogenic or likely pathogenic by InterVar, CADD >25, and protein variation effect analyzer <-2.5.

RNA Sequencing Analysis

Total RNA was extracted from cultured CFs when they were subconfluent using a NucleoSpin RNA column kit. Library preparation was performed using the TruSeq stranded mRNA sample prep kit (Illumina). Sequencing was performed on an Illumina HiSeq 2500 platform in 75-base single-end mode. The Illumina CASAVA 1.8.2 software was used for base calling.

Sequenced reads were mapped to the human reference genome sequence (hg 19) using TopHat version 2.0.13 in combination with Bowtie2 version 2.2.3 and SAMtools version 0.1.19. Fragments per kilobase of exon per million mapped fragments were calculated using Cuffnorm version 2.2.1. Ingenuity pathway analysis was used to identify canonical pathways from differentially expressed genes. Access to the study data may be found under Gene Expression Omnibus (GEO) experiment accession number (GEO223517). The CF transcriptomes obtained from patients with DCM and healthy CFs were analyzed via the Subio platform (Subio) and integrated Differential Expression and Pathway analysis for bulk RNA-seq. Single-cell RNA-seq data were analyzed by using the Loupe cell browser (10x Genomics, Pleasanton, CA).^{25,26} In addition, the list of the enriched Kyoto Encyclopedia of Genes and Genomes pathways were obtained using the DAVID functional annotation web tool (<https://david-d.ncifcrf.gov>). For single-cell RNA sequences, we used 2 DCM lines and a healthy control sample.

Atomic Force Microscopy Measurements

We used multifrequency force modulation atomic force microscopy,²⁷ with a rectangular cantilever with a sharp tip (BioLever mini, BL-AC40TSC2; Olympus, Tokyo, Japan), to measure the complex shear modulus, G^* , of CFs around the center of the cells. The measured G^* was fitted to the power-law structural damping model with additional Newtonian viscosity²⁸ given by

$$G^* = G_0 g(\alpha) \{1 + i \eta(\alpha)\} \left(\frac{f}{f_0} \right) + i \mu f,$$

where α is the power-law exponent between 0 for solid and 1 for liquid. $g(\alpha)$ is $\Gamma(1-\alpha) \cos(\pi\alpha/2)$, with Γ denoting the gamma function. G_0 is the scale factor of the modulus at a frequency scale factor f_0 , which was arbitrarily set to 1 Hz. The hysteresivity $\eta(\alpha)$ is equivalent to $\tan(\pi\alpha/2)$, and μ is the Newtonian viscous damping coefficient. The detailed methods for evaluating the rheology of CFs are described elsewhere.²⁰

Statistical Analysis

All data are expressed as the mean±SE. All statistical analyses were performed with Easy R (Saitama Medical Centre, Jichi Medical University; <http://www.jichi.ac.jp/saitama-sct/SaitamaHP.files/statmedEN.html>; Kanda²⁹), which is a graphical user interface for R (The R Foundation for Statistical Computing, Vienna, Austria; version 2.13.0. from Jichi Medical University, Tochigi, Japan). An unpaired t test was performed using a 2-group comparison. P values <0.05 were considered statistically significant.

RESULTS

Clinical Characteristics of the Patients

The clinical profiles of the patients are listed in the Table. Two patients were boys, and 2 were girls. They were diagnosed as DCM from 2 months to 8 years old. Cardiac specimens were obtained from the free wall of the left ventricle from patients receiving heart transplantation between the ages of 2 and 16 years. Two patients had implanted left ventricular assist devices before transplantation. DCM 1 exhibited a pathogenic missense variant in the *TNNT2* gene, which was reported to cause DCM in a previous report.³⁰ In the other 3 patients, there was no candidate variant detected via whole exome sequence, including variants of unknown significance in cardiomyopathy-associated genes. Echocardiographic images and histological images of Masson trichrome-stained specimens are shown in Figure 1. The fibrotic area ratio was not significantly different among patients.

Physiological Features of CFs Derived From the Pediatric Patients With DCM

We initially evaluated cell proliferation, migration, attachment, apoptosis, and myofibroblast activation in DCM patient-derived CFs. There was no significant difference between healthy CFs (HCFs) and DCM CFs with respect to proliferation (0.39 ± 0.05 versus 0.43 ± 0.02 , $P=0.54$; Figure 2A), migration (0.28 ± 0.08 versus 0.35 ± 0.37 , $P=0.50$; Figure 2B), or attachment (251.7 ± 45.2 versus 244.2 ± 16.2 , $P=0.88$; Figure 2C). Next, we evaluated apoptosis in CFs and α -smooth muscle actin-positive CFs, known as myofibroblasts, under 4 experimental conditions, including with or without hypoxia and serum deprivation. There were no significant differences in the ratio of apoptosis or activated myofibroblasts under any conditions (Figure 2D and 2E). Finally, cellular rheology of DCM CFs was measured by atomic force microscopy, because we previously found significant changes

in stiffness, viscosity, and fluidity in CFs derived from pediatric RCM patients.²⁰ However, there were no significant differences between HCFs and DCM CFs in cellular stiffness (G_0 ; 2.55 ± 0.13 versus 2.72 ± 0.08 , $P=0.078$; Figure 2F), viscosity (α ; 0.267 ± 0.005 versus 0.246 ± 0.011 , $P=0.169$; Figure 2G), or fluidity (μ ; 0.130 ± 0.012 versus 0.183 ± 0.029 , $P=0.347$; Figure 2H). Collectively, we could not identify any significant differences between HCFs and DCM CFs in these cellular physiological and rheological characteristics.

Contractile and Diastolic Functions of Healthy Cardiomyocytes Are Impaired by Coculture With DCM CFs

To examine the interaction between CFs and cardiomyocytes through paracrine effects and direct cell-cell interaction, we performed indirect and direct coculture assays of healthy cardiomyocytes and CFs. We evaluated the motion vectors of beating cardiomyocytes after 48 hours of coculture with HCFs and DCM CFs using a Sony SI8000 motion analyzer. The motion vector analysis has previously been demonstrated to quantitatively represent the electrophysiological and functional characteristics of cardiomyocytes.^{31,32} In the indirect coculture assay, the beating rate and contraction velocity of cardiomyocytes cocultured with CFs derived from healthy controls or patients with DCM were not significantly different (66.8 ± 9.3 versus 79.6 ± 11.6 , $P=0.076$; Figure 3A; 10.4 ± 0.81 versus 8.4 ± 0.38 , $P=0.131$; Figure 3B). In contrast, the relaxation velocity of cardiomyocytes cocultured with DCM CFs was significantly lower compared with that of coculture with HCFs (6.7 ± 0.27 versus 5.6 ± 0.28 , $P=0.0496$; Figure 3C). The expression levels of *Nppa*, *Nppb*, *Myh7*, *Myh6*, *Myl2*, *Actc1*, *Tnnt2*, *Atp2a2*, *Pln*, and *Gja1*, which might be associated with cardiomyocyte contractility, were not significantly changed in the cardiomyocytes, which were indirectly cocultured with DCM CFs (Figure 3D).

Table. Clinical Characteristics of the Patients

Characteristic	DCM 1	DCM 2	DCM 3	DCM 4
Sex	Girl	Boy	Girl	Boy
Age at diagnosis	1 y	2 mo	8 y	4 mo
Age at sampling, y	4	4	16	2
Event at sampling	HTx	HTx	HTx	HTx
Medications at sampling	Milrinone Diuretics ACE inhibitor β -blocker	Milrinone Diuretics ACE inhibitor β -blocker	LVAD Diuretics Warfarin	LVAD Diuretics Warfarin ACE inhibitor β -blocker
BNP at sampling	257.5 pg/mL	63.7 pg/mL	53.9 pg/mL	180.6 pg/mL
Gene variant	<i>TNNT2</i> (R141W)	Not detected	Not detected	Not detected

ACE indicates angiotensin-converting enzyme; BNP, B-type natriuretic peptide; DCM, dilated cardiomyopathy; HTx, heart transplantation; and LVAD, left ventricular assist device.

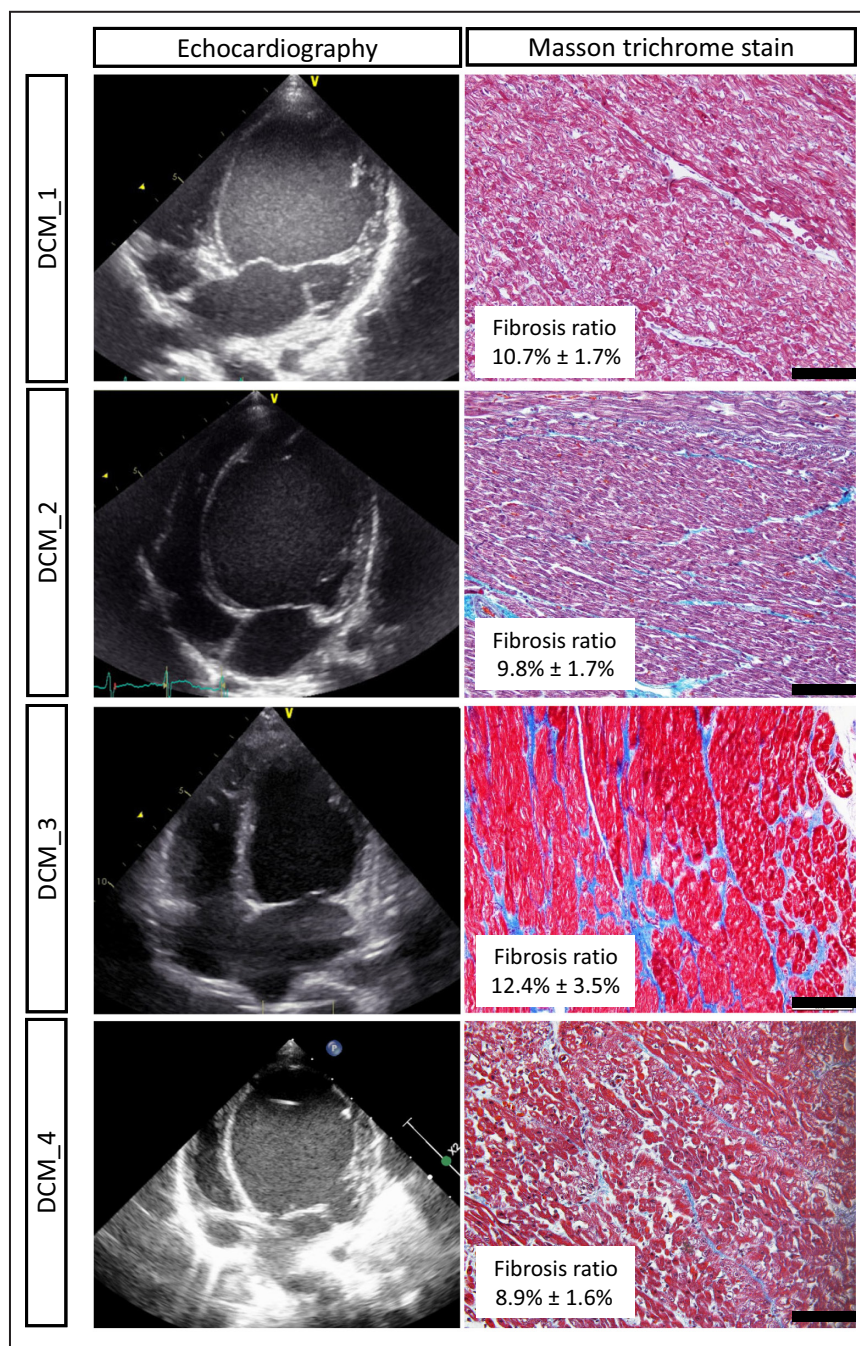


Figure 1. Clinical echocardiographic and histological data of the patients.

Echocardiographic findings of patients demonstrating dilated left ventricles. Masson trichrome staining of cardiac tissue from the left ventricle free wall indicates mild interstitial fibrosis (blue stain). The fibrosis ratio was evaluated at 5 different locations in the sections and was not significantly different among patients. Scale bar: 200 μ m. DCM indicates dilated cardiomyopathy.

In the direct coculture assay, although the beating rate of cardiomyocytes cocultured with DCM CFs was not significantly changed (70.2 ± 6.9 versus 65.3 ± 1.2 , $P=0.626$; Figure 4A), the contraction velocity and relaxation velocity of cardiomyocytes cocultured with DCM CFs were significantly lower compared with those cocultured with

HCFs (14.7 ± 0.43 versus 11.0 ± 0.37 , $P=0.0375$; Figure 4B; 9.7 ± 0.27 versus 7.2 ± 0.19 , $P=0.0207$; Figure 4C). The expression levels of *Nppa*, *Nppb*, *Myh7*, *Myh6*, *Myl2*, *Actc1*, *Tnnt2*, *Atp2a2*, *Pln*, and *Gja1* were not significantly changed between the cardiomyocytes cocultured with HCFs and DCM CFs (Figure 4D).

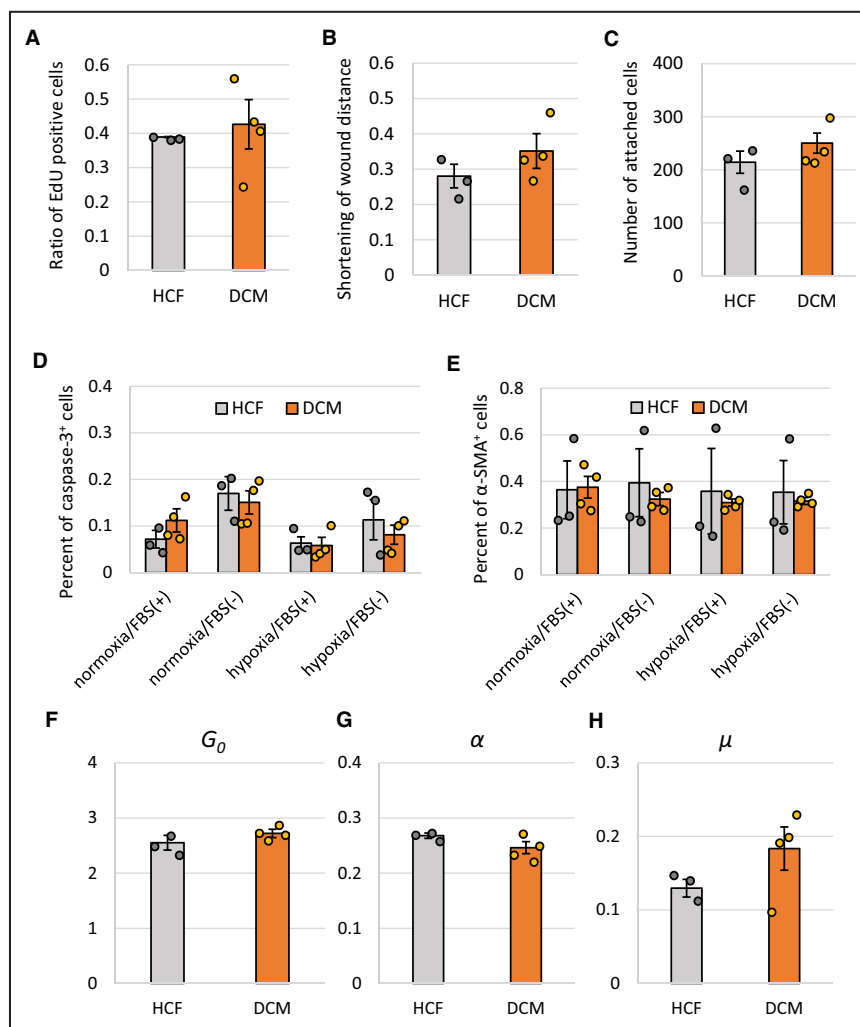


Figure 2. Cellular physiological assays of cardiac fibroblasts (CFs) derived from patients with dilated cardiomyopathy (DCM) and healthy controls.

Three independent experiments were conducted for each patient for all experiments. The mean values and SEs were calculated from 3 different lines of healthy cardiac fibroblasts (HCFs) and 4 different DCM patient-derived CFs. **A**, Proliferation assay measuring the number of EdU-positive cells. There was no significant difference between HCFs and DCM CFs. **B**, A migration assay was performed by measuring the wound dimensions after scratching the cell culture dishes. There was no significant difference between HCFs and DCM CFs. **C**, The results of the cell attachment assay indicates no significant difference. **D**, Apoptosis assay was done by counting the cleaved caspase-3-positive cells under a combination of hypoxia and serum starvation conditions. There were no significant differences between HCFs and DCM CFs. **E**, The myofibroblast activation assay was done by counting the α -smooth muscle actin-positive CFs under a combination of hypoxia and serum starvation conditions. There were no significant differences between HCFs and DCM CFs. The cell modulus scale factor, G_0 (**F**), the power-law exponent, α (**G**), the Newtonian viscous damping coefficient, μ (**H**) in CFs derived from patients with HCFs and DCM CFs, which were measured by atomic force microscopy. There were no significant differences between HCFs and DCM CFs.

RNA Sequencing Analysis

To determine how DCM CFs may affect the contractile and diastolic functions of cardiomyocytes, we performed the RNA sequencing analysis to establish comprehensive expression profiles for CFs. A heat map analysis of the top 2000 genes revealed distinct

expression patterns between HCFs and DCM CFs (Figure 5A). K-means clustering divided the top 1000 genes into 3 groups and also showed similar distinctive expression patterns (Figure 5B). A gene ontology term analysis revealed that pathways associated with cardiovascular development, cardiac muscle development,

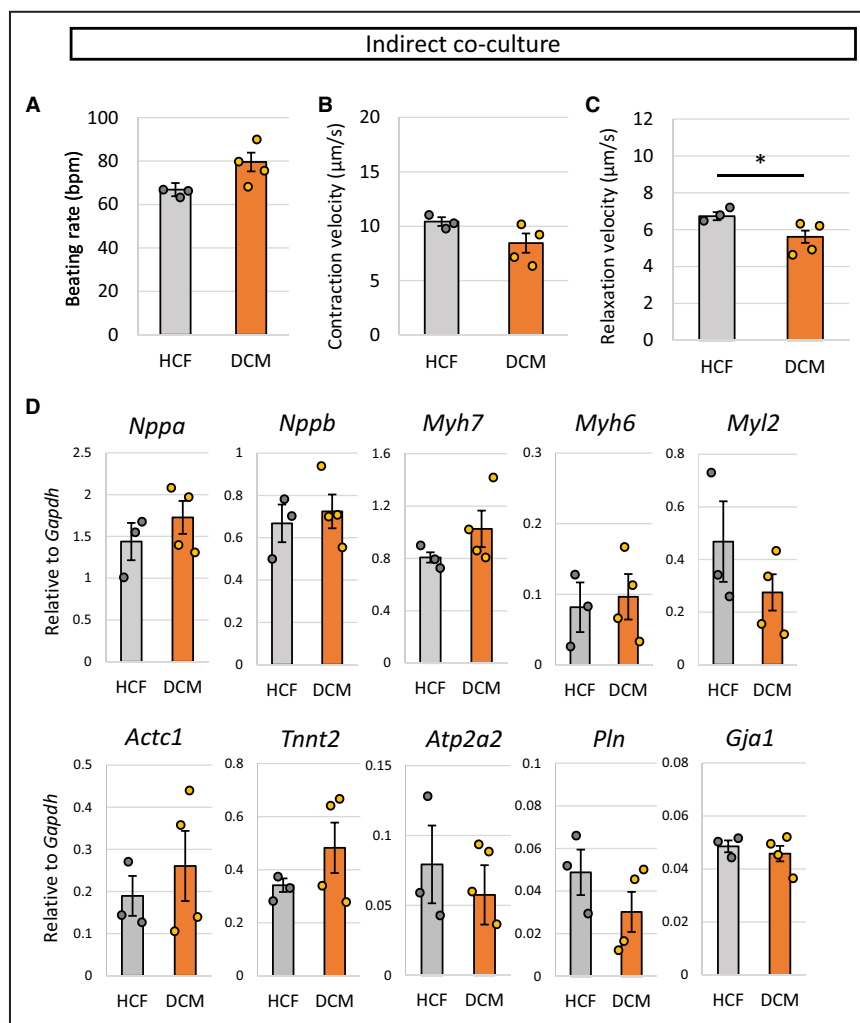


Figure 3. Indirect coculture assays of cardiac fibroblasts (CFs) with healthy rat cardiomyocytes.

Three independent coculture experiments were conducted for each patient. Ten to 20 beating cells were assayed in 1 experiment. The mean values were calculated from 3 different lines of healthy cardiac fibroblasts (HCFs) and 4 different dilated cardiomyopathy (DCM) patient-derived CFs. The graphs show the mean \pm SE. **A through C**, Motion analyses of healthy cardiomyocytes under indirect coculture conditions with HCFs and DCM CFs. * $P < 0.05$. **D**, Quantitative polymerase chain reaction analyses for contractility-related genes of rat cardiomyocytes indirectly cocultured with CFs. There were no significant differences in all genes between the cardiomyocytes cocultured with HCF and DCM CFs.

and extracellular cellular structure and stimuli were enriched in each cluster (Figure S1). Moreover, pathways of cardiomyopathy-associated genes were enriched in each cluster by Kyoto Encyclopedia of Genes and Genomes analysis (Figure S2). Principal component analysis clearly demonstrated the distinct grouping of HCFs and DCM CFs, indicating that DCM CFs have unique gene expression patterns compared with HCFs, and these expression patterns were maintained even under in vitro culture conditions (Figure 5C). Interestingly, there was no apparent difference in the expression profiles in DCM 1, which harbored a *TNNT2* pathogenic variant, compared with DCM 2, 3,

and 4, which exhibited no candidate pathogenic variants (Figure 5A through 5C).

We performed pathway analysis to determine which particular signaling pathways influenced cardiomyocyte behaviors. ECM receptor interactions ($P = 0.000173$) and the focal adhesion signaling cascade ($P = 0.00505$) were found to be considerably active in DCM CFs. Furthermore, the Hippo signaling pathway ($P = 0.000845$) and the transforming growth factor (TGF)- β pathway ($P = 0.0116$) were substantially altered (Figure S3). Then, we evaluated the expression levels of collagen, fibronectin, α -smooth muscle cell actin, and TGF- β -related genes (Figure S4).

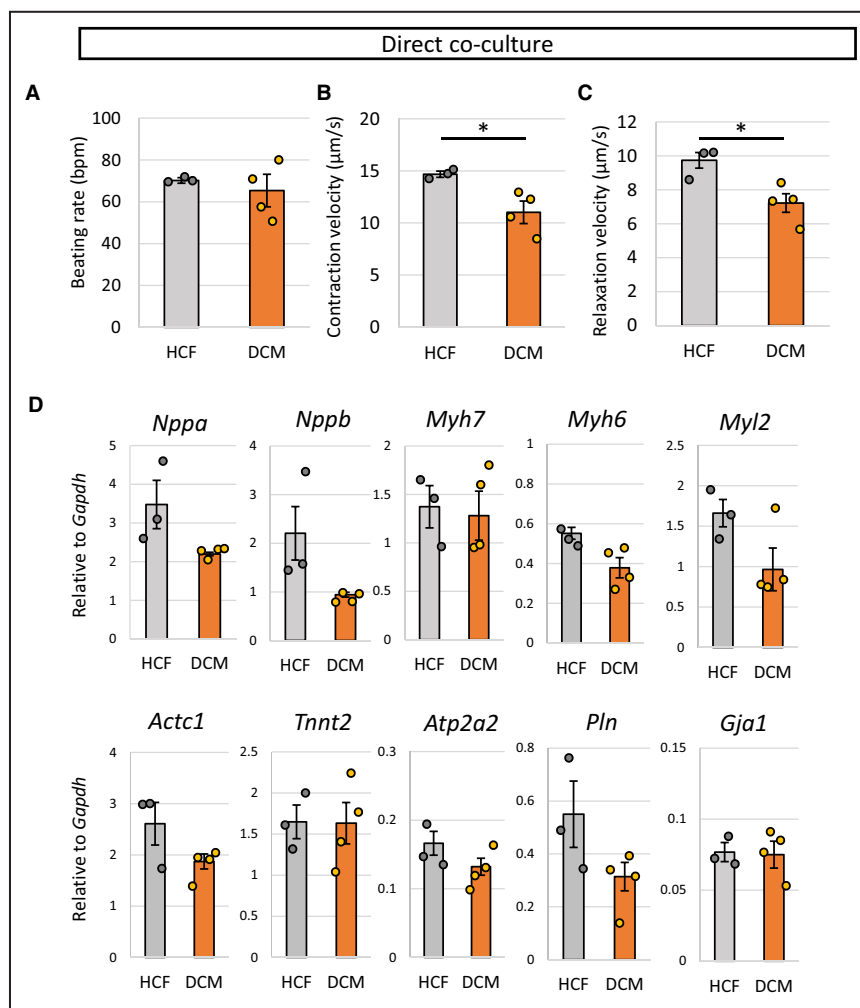


Figure 4. Direct coculture assays of patient-derived cardiac fibroblasts (CFs) and healthy rat cardiomyocytes.

Three independent coculture experiments were conducted for each patient. Thirty to 40 beating cells were assayed in 1 experiment. The mean values were calculated from 3 different lines of healthy cardiac fibroblasts (HCFs) and 4 different dilated cardiomyopathy (DCM) patient-derived CFs. The graphs show the mean \pm SE. **A** through **C**, Motion analysis under direct coculture conditions. **D**, Quantitative polymerase chain reaction analyses for contractility-related genes of rat cardiomyocytes directly cocultured with CFs using rat-specific primers. There were no significant differences in all genes between the HCF and DCM CF coculture assays. * $P < 0.05$.

Several forms of collagen, including *COL1A1*, *COL1A2*, *COL5A1*, *COL5A2*, and *COL16A1* were elevated, whereas laminin gene expression (*LAMA4* and *LAMB1*) were discovered to be downregulated. *FN1* (fibronectin) and *ACTA2* (α -smooth muscle cell actin) expressions were not altered. In terms of TGF- β signaling, *TGFB1*, *BAMBI*, and *SMAD3* expression levels were considerably greater in DCM CFs than in healthy CFs, although *TGFB1*, *SMAD6*, and *SMAD7* expression levels were not statistically different. Using the DESeq2 package with a threshold false discovery rate < 0.1 and fold change > 2 , we identified 620 upregulated and 545 downregulated genes in the DCM CF group

compared with the HCF group. The altered expression of several genes that were reported to be associated with cardiac function and mechanical interactions, including *ITGA11*, *COL16A1*, *CDH2*, *TGFB1*, *COL1A1*, and *FGF2*, were significantly higher in DCM CFs compared with healthy CFs. In contrast, the expression levels of *CXCL12* and *IL33* were significantly lower in DCM CFs compared with healthy CFs (Figure 5D).

Finally, we conducted single-cell RNA sequencing analysis to identify the subpopulation of CFs that may be responsible for the alterations in gene expression, because fibroblasts are not uniform cell populations.³³ Unsupervised uniform manifold approximation and

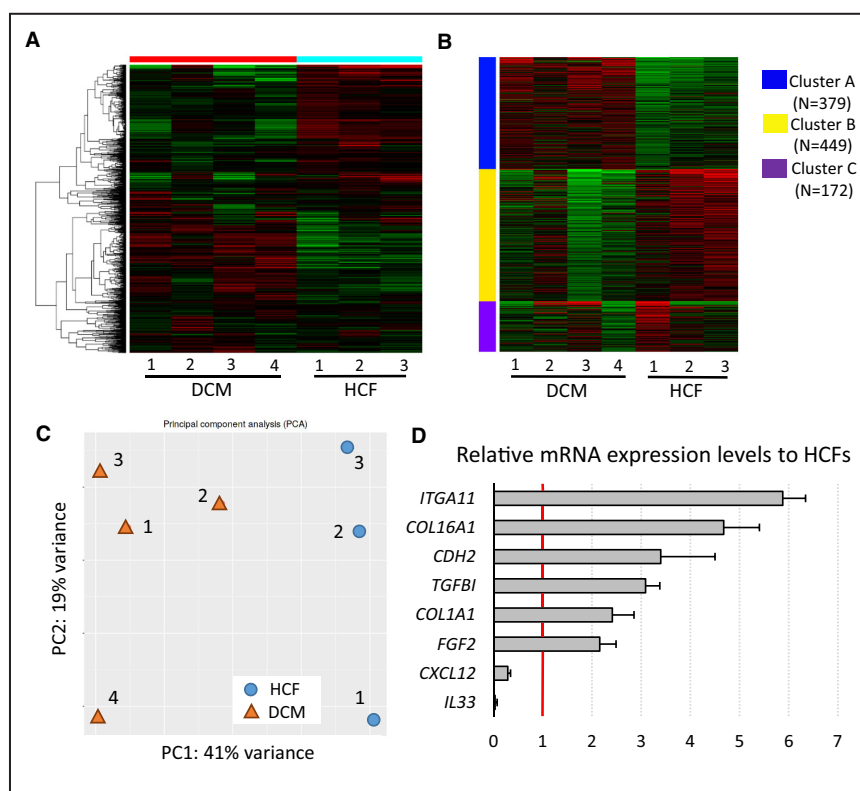


Figure 5. RNA sequencing analyses for cardiac fibroblasts (CFs) derived from patients with dilated cardiomyopathy (DCM) and healthy controls.

A, Hierarchical clustering of RNA sequencing in healthy control fibroblasts (HCFs) and DCM CFs. **B**, K-means clustering analysis of the top 1000 differentially expressed genes. **C**, Principal component (PC) analysis of RNA-sequencing. Each number represents each DCM patient and healthy control. **D**, Differential gene expression analysis showing that the expression levels of *ITGA11*, *COL16A1*, *CDH2*, *TGFB1*, *COL1A1*, and *FGF2* were significantly elevated in DCM CFs compared with HCFs. In contrast, *CXCL12* and *IL33* were significantly downregulated in DCM CFs.

projection clustering analyses revealed that there were 10 to 14 distinctive clusters in each CF line from healthy controls and patients with DCM (Figure S5A). The integrated uniform manifold approximation and projection data set showed 2 DCM CF lines from independent patients had distinctive clusters, which were distinctive from those of HCFs (Figure S5B). We confirmed that the altered expression levels in the bulk RNA sequencing data were also observed in single-cell RNA sequencing (Figure 6A). However, we could not identify any specific subpopulations that might contribute to the change of gene expression levels in DCM CFs. This suggests that the altered expression of several specific genes was attributed to the entire population of DCM CFs (Figure 6B).

DISCUSSION

Pediatric cardiomyopathy is a rare disease; however, the prognosis is generally poor.¹ Cardiomyocytes have been implicated in the underlying cause, and some

causative genes have been identified. However, not all causes can be explained by gene mutations in cardiomyocytes. Thus, it is important to consider other types of cells rather than cardiomyocytes to fully elucidate the pathogenesis of cardiomyopathy. CFs have been implicated as one such target; however, experiments using human CFs are limited because of sample scarcity. Therefore, their role in cardiomyopathy remains unclear.

In the present study, we demonstrated that CFs derived from pediatric patients with DCM can deteriorate cardiomyocyte dilatation through humoral factors and direct cell–cell contact, and deteriorate contractile function via direct contact. These results suggest that DCM CFs play a pathological role in DCM, although other physiological behaviors were not significantly affected. Interestingly, we identified significant differences in contractile velocity in direct coculture, whereas we did not observe significant impairment of cardiomyocyte contraction under indirect coculture conditions. Thus, we hypothesized that direct CF–cardiomyocyte interaction

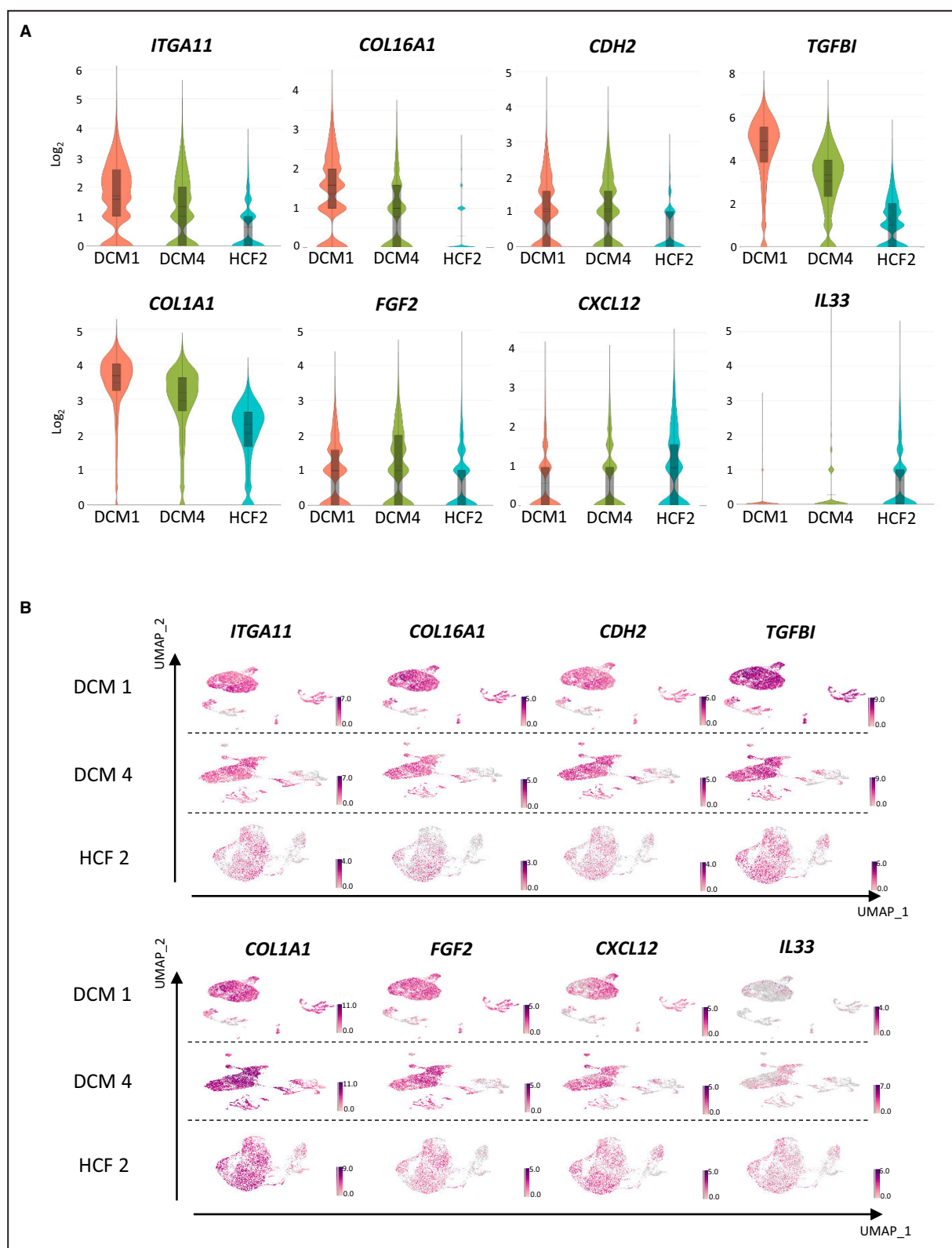


Figure 6. Single-cell RNA sequencing analyses for cardiac fibroblasts (CFs) derived from patients with dilated cardiomyopathy (DCM) and healthy controls.

A, Violin plot analyses of genes that were identified in bulk RNA sequencing shown in Figure 5D. **B**, Unsupervised uniform manifold approximation and projection (UMAP) clustering of single CFs derived from DCM 1, DCM 4, and healthy control fibroblasts (HCFs) 2.

or ECM secreted from CFs may be more important for DCM pathogenesis. It is well recognized that cancer-associated fibroblasts regulate the biological behavior of tumor cells via cell–cell contact and remodeling of ECM.³⁴ Thus, we examined the cellular rheological alterations using atomic force microscopy. In a previous study, we demonstrated that CFs derived from pediatric RCM patients exhibited higher stiffness and viscosity with lower cellular fluidity.²⁰ However, in the present study, we did not observe any significant differences in cellular stiffness, fluidity, or viscosity in DCM CFs, suggesting that the rheological properties of CFs do not affect the behavior of DCM cardiomyocytes, and they are different according to the type of cardiomyopathy. RCM is characterized by preserved ventricular contraction with diastolic dysfunction. The ventricle becomes stiff in the absence of severe fibrosis and hypertrophy in the heart. Conversely, DCM is characterized by impaired contraction and a dilated ventricle. The ventricle becomes thin as its contractility decreases. RCM and DCM have considerably diverse cardiac phenotypes, despite the fact that both disorders are categorized as cardiomyopathy. The properties of RCM CFs and DCM CFs are similar in some ways but distinct in others. Both CFs exhibited higher expression levels of ECM, which could affect cardiomyocyte behavior. RCM CFs can deteriorate the diastolic function of healthy cardiomyocytes and show higher stiffness and viscosity with lower fluidity.^{19,20} DCM CFs showed no rheological changes as revealed by atomic force microscopy but could deteriorate contraction and relaxation in healthy cardiomyocytes by modulating ECM structures, focal adhesion signaling, and humoral factors. These differences in disease-associated CFs might be a potential cause of differential pathogenicity in different types of cardiomyopathy.

We also demonstrated by RNA sequencing analysis that DCM CFs had a distinctive gene expression profile compared with healthy CFs. This result was similar to that of our previous study, in which we demonstrated that CFs from RCM patients impaired the function of normal cardiomyocytes,¹⁹ suggesting that abnormal hemodynamic situations and mechanical stresses may alter the gene expression profiles of CFs in cardiomyopathy patients. Moreover, such abnormal expression profiles are maintained even in *in vitro* situations. A recent single-cell RNA sequencing study of adult patients with DCM revealed that the expression profiles of cardiomyocytes as well as other cell types, including CFs, endothelial cells, and immunological cells, were significantly altered in DCM hearts compared with healthy controls.³³

Next, to identify specific signaling pathways causing the dysregulation of cardiomyocyte behavior, we conducted the pathway analyses and differential gene expression analyses. The pathway analyses indicated that focal adhesion signaling and ECM receptor interaction were significantly changed in DCM CFs. Additionally, Hippo

signaling and TGF- β signaling pathways were also altered in DCM CFs. The Hippo pathway has been reported to play various important roles in myocardial infarction and cardiomyopathy.³⁵ Especially, *Lats1/2* and *Yap* knock-down in CFs induce fibrotic and proinflammatory cascade in the infarcted models.^{36,37} TGF- β signaling is also reported to be activated in the experimental models of myocardial infarction, cardiac hypertrophy, and in human patients with DCM.³⁸ Therefore, it is suggested that these multiple pathways can impair the cardiomyocyte contractility. The differential gene expression analyses also identified the alteration of more specific gene expressions; *ITGA11*, *COL16A1*, *CDH2*, *TGFBI*, *COL1A1*, and *FGF2* were significantly upregulated, whereas *CXCL12* and *IL33* were significantly downregulated. These genes have been shown to be associated with the pathogenesis of heart disease in previous studies using various models.^{39–41} Of these, *CXCL12* and *IL33* have antifibrotic or protective effects,^{42,43} whereas TGF- β signaling is involved in cardiac fibrosis and fibroblast activation.^{44–46} As previously reported, both *TGFBI* and *FGF2* are involved in increased expression of focal adhesion and ECM proteins, such as *ITGA11*, *CDH2*, *COL16A1*, and *COL1A1*.^{47–49} Increased focal adhesion, and ECM proteins may alter cell–cell interactions and affect the contractile and diastolic behaviors of cardiomyocytes. Moreover, the lack of antifibrotic and protective factors may accelerate the detrimental effects on cardiomyocytes. Although we could not identify which specific signaling pathway mainly contributes to the impairment of cardiomyocyte function, we speculated that multiple signaling pathways via humoral factors, adhesion proteins, and ECM may be involved in the pathogenicity of DCM. In addition, we conducted single-cell RNA sequencing to determine whether the differential gene expression analysis identified in DCM CFs were caused by a rearrangement of specific subpopulations of CFs. A recent study using single cell transcriptomics found that CFs harvested from patients with DCM exhibited a dramatic diversification in CF populations.³³ Similarly, we found that several subpopulations existed in CFs, which reflect their heterogeneity. However, focusing on the expression levels of the aforementioned candidate genes, there was no obvious subpopulation that contributed to the drastic alteration in gene expression levels. These results suggest that the specific expression patterns in DCM CFs were attributed to common features of DCM CFs and not to a specific subpopulation of CFs. Conversely, when we focused on the gene expression patterns in cardiomyocytes, we did not identify any significant changes in the expression levels of sarcomere, gap junction, and calcium handling–associated genes. We speculate that the reduced contractility of healthy cardiomyocytes cocultured with DCM CFs was not associated with the changes in mRNA expressions of sarcomere, calcium handling, and gap junction. Further study is required to determine which specific signaling pathways

primarily contribute to cardiomyocyte contractility impairment and how contractility is disrupted in cardiomyocytes cocultured with DCM CFs.

One limitation to this study was the small number of DCM CF cell lines available. In addition, we used rat, not human, cardiomyocytes for these experiments. Because species differences may be a limitation, coculture experiments using induced pluripotent stem cell–derived cardiomyocytes will be conducted in the future. In addition, the age and race of healthy and DCM CFs are distinct. There is no evidence that the cellular physiology and gene expression profiles of CFs differ among races; however, race-related differences cannot be ruled out. Despite the fact that healthy CFs are derived from youthful, healthy adults, this may be a minor limitation of the study.

In conclusion, DCM patient-derived CFs demonstrate distinct expression patterns from those of healthy CFs and are involved in the pathogenesis of DCM via humoral factors and direct cell–cell interactions, which affect the contractile and diastolic function of cardiomyocytes.

ARTICLE INFORMATION

Received February 1, 2023; accepted May 24, 2023.

Affiliations

Department of Pediatrics, Osaka University Graduate School of Medicine, Osaka, Japan (H.T., C.Y., H.S., J.N., R.I., R.W., A.U., K.U., M.H., K.H., H.N., K.O., H.I.); Department of Pediatrics, Niigata University School of Medicine, Niigata, Japan (H.T.); Graduate School of Information Science and Technology, Hokkaido University, Sapporo, Japan (M.M., R.T., T.O.); and Department of Pediatric Cardiology, Osaka Medical Center for Maternal and Child Health, Osaka, Japan (Y.I.).

Acknowledgments

The authors thank Dr Miyashita and Dr Asano, Department of Cardiology, Osaka University Graduate School of Medicine, for the kind help with whole exome sequence analysis. H.T., C.Y., H.S., R.W., and K.U. conducted the cell experiments. M.M., R.T., and T.O. performed the atomic force microscopy experiments. J.N., R.I., M.H., K.H., and H.N. collected the clinical samples and prepared them for the initial procedures. H.T., C.Y., A.U., and H.I. analyzed the RNA-seq data. Y.I. conducted pathway analyses. H.T., H.I., and K.O. designed all of the experimental procedures. H.I., H.T., T.O. wrote the article, and all authors revised and approved the final version of the article.

Sources of Funding

This study was supported by grants from the Ministry of Education, Science, Sports, and Culture of Japan (number 18K07789 and 21K07749).

Disclosures

None.

Supplemental Material

Table S1
Figures S1–S5

REFERENCES

- Lee TM, Hsu DT, Kantor P, Towbin JA, Ware SM, Colan SD, Chung WK, Jefferies JL, Rossano JW, Castleberry CD, et al. Pediatric cardiomyopathies. *Circ Res*. 2017;121:855–873. doi: 10.1161/CIRCRESAHA.116.309386
- Schultheiss HP, Fairweather D, Caforio ALP, Escher F, Hersberger RE, Lipshultz SE, Liu PP, Matsumori A, Mazzanti A, McMurray J, et al. Dilated cardiomyopathy. *Nat Rev Dis Primers*. 2019;5:32. doi: 10.1038/s41572-019-0084-1
- Ware SM. Evaluation of genetic causes of cardiomyopathy in childhood. *Cardiol Young*. 2015;25(suppl 2):43–50. doi: 10.1017/S1047951115000827
- Tariq M, Ware SM. Importance of genetic evaluation and testing in pediatric cardiomyopathy. *World J Cardiol*. 2014;6:1156–1165. doi: 10.4330/wjc.v6.i11.1156
- Forleo C, D'Erchia AM, Sorrentino S, Manzari C, Chiara M, Iacoviello M, Guaricci AI, Santis DD, Musci RL, Spada AL, et al. Targeted next-generation sequencing detects novel gene-phenotype associations and expands the mutational spectrum in cardiomyopathies. *PLoS One*. 2017;12:e0181842. doi: 10.1371/journal.pone.0181842
- Ellepolu CD, Knight LM, Fischbach P, Deshpande SR. Genetic testing in pediatric cardiomyopathy. *Pediatr Cardiol*. 2018;39:491–500. doi: 10.1007/s00246-017-1779-2
- Mogensen J, Hey T, Lambrecht S. A systematic review of phenotypic features associated with cardiac troponin I mutations in hereditary cardiomyopathies. *Can J Cardiol*. 2015;31:1377–1385. doi: 10.1016/j.cjca.2015.06.015
- Arbustini E, Narula N, Dec GW, Reddy KS, Greenberg B, Kushwaha S, Marwick T, Pinney S, Bellazzi R, Favalli V, et al. The MOGE(S) classification for a phenotype-genotype nomenclature of cardiomyopathy: endorsed by the World Heart Federation. *J Am Coll Cardiol*. 2013;62:2046–2072. doi: 10.1016/j.jacc.2013.08.1644
- Bagnall RD, Singer ES, Wacker J, Nowak N, Ingles J, King I, Macciocca I, Crowe J, Ronan A, Weintraub RG, et al. Genetic basis of childhood cardiomyopathy. *Circ Genom Precis Med*. 2022;15:e003686. doi: 10.1161/CIRCGEN.121.003686
- Baudino TA, Carver W, Giles W, Borg TK. Cardiac fibroblasts: friend or foe? *Am J Physiol Heart Circ Physiol*. 2006;291:H1015–H1026. doi: 10.1152/ajpheart.00023.2006
- Camelliti P, Borg TK, Kohl P. Structural and functional characterisation of cardiac fibroblasts. *Cardiovasc Res*. 2005;65:40–51. doi: 10.1016/j.cardiores.2004.08.020
- Souders CA, Bowers SL, Baudino TA. Cardiac fibroblast: the renaissance cell. *Circ Res*. 2009;105:1164–1176. doi: 10.1161/CIRCRESAHA.109.209809
- Ieda M, Tsuchihashi T, Ivey KN, Ross RS, Hong TT, Shaw RM, Srivastava D. Cardiac fibroblasts regulate myocardial proliferation through beta1 integrin signaling. *Dev Cell*. 2009;16:233–244. doi: 10.1016/j.devcel.2008.12.007
- Deb A, Ubil E. Cardiac fibroblast in development and wound healing. *J Mol Cell Cardiol*. 2014;70:47–55. doi: 10.1016/j.yjmcc.2014.02.017
- Kakkar R, Lee RT. Intramyocardial fibroblast myocyte communication. *Circ Res*. 2010;106:47–57. doi: 10.1161/CIRCRESAHA.109.207456
- Khalil H, Kanisicak O, Prasad V, Correll RN, Fu X, Schips T, Vagnozzi RJ, Liu R, Huynh T, Lee SJ, et al. Fibroblast-specific TGF-beta-Smad2/3 signaling underlies cardiac fibrosis. *J Clin Invest*. 2017;127:3770–3783. doi: 10.1172/JCI94753
- Quaife-Ryan GA, Sim CB, Ziemann M, Kaspi A, Rafehi H, Ramalison M, El-Osta A, Hudson JE, Porrello ER. Multicellular transcriptional analysis of mammalian heart regeneration. *Circulation*. 2017;136:1123–1139. doi: 10.1161/CIRCULATIONAHA.117.028252
- Le Bras A. Dynamics of fibroblast activation in the infarcted heart. *Nat Rev Cardiol*. 2018;15:379. doi: 10.1038/s41569-018-0025-9
- Tsuru H, Ishida H, Narita J, Ishii R, Suginohe H, Ishii Y, Wang R, Kogaki S, Taira M, Ueno T, et al. Cardiac fibroblasts play pathogenic roles in idiopathic restrictive cardiomyopathy. *Circ J*. 2021;85:677–686. doi: 10.1253/circ.CJ-20-1008
- Matsumoto M, Tsuru H, Suginohe H, Narita J, Ishii R, Hirose M, Hashimoto K, Wang R, Yoshihara C, Ueyama A, et al. Atomic force microscopy identifies the alteration of rheological properties of the cardiac fibroblasts in idiopathic restrictive cardiomyopathy. *PLoS One*. 2022;17:e0275296. doi: 10.1371/journal.pone.0275296
- Beeres SL, Atsma DE, van der Laarse A, Pijnappels DA, van Tuyn J, Fibbe WE, de Vries AAF, Ypey DL, van der Wall EE, Schalij MJ. Human adult bone marrow mesenchymal stem cells repair experimental conduction block in rat cardiomyocyte cultures. *J Am Coll Cardiol*. 2005;46:1943–1952. doi: 10.1016/j.jacc.2005.07.055

22. Simpson P, Savion S. Differentiation of rat myocytes in single cell cultures with and without proliferating nonmyocardial cells. Cross-striations, ultrastructure, and chronotropic response to isoproterenol. *Circ Res*. 1982;50:101–116. doi: 10.1161/01.RES.50.1.101
23. Shibamoto M, Higo T, Naito AT, Nakagawa A, Sumida T, Okada K, Sakai T, Kuramoto Y, Yamaguchi T, Ito M, et al. Activation of DNA damage response and cellular senescence in cardiac fibroblasts limit cardiac fibrosis after myocardial infarction. *Int Heart J*. 2019;60:944–957. doi: 10.1536/ihj.18-701
24. Ito M, Hara H, Takeda N, Nakagawa A, Sumida T, Okada K, Sakai T, Kuramoto Y, Yamaguchi T, Ito M, et al. Characterization of a small molecule that promotes cell cycle activation of human induced pluripotent stem cell-derived cardiomyocytes. *J Mol Cell Cardiol*. 2019;128:90–95. doi: 10.1016/j.jmcc.2019.01.020
25. Ge SX, Son EW, Yao R. iDEP: an integrated web application for differential expression and pathway analysis of RNA-Seq data. *BMC Bioinform*. 2018;19:534. doi: 10.1186/s12859-018-2486-6
26. Saji H, Tsuboi M, Shimada Y, Kato Y, Hamanaka W, Kudo Y, Yoshida K, Matsubayashi J, Usuda J, Ohira T, et al. Gene expression profiling and molecular pathway analysis for the identification of early-stage lung adenocarcinoma patients at risk for early recurrence. *Oncol Rep*. 2013;29:1902–1906. doi: 10.3892/or.2013.2332
27. Takahashi R, Okajima T. Mapping power-law rheology of living cells using multi-frequency force modulation atomic force microscopy. *Appl Phys Lett*. 2015;107:173702. doi: 10.1063/1.4934874
28. Kollmannsberger P, Fabry B. Linear and nonlinear rheology of living cells. *Annu Rev Mater Res*. 2011;41:75–97. doi: 10.1146/annurev-matsci-062910-100351
29. Kanda Y. Investigation of the freely available easy-to-use software 'EZR' for medical statistics. *Bone Marrow Transplant*. 2013;48:452–458. doi: 10.1038/bmt.2012.244
30. Ramratnam M, Salama G, Sharma RK, Wang DRW, Smith SH, Banerjee SK, Huang XN, Gifford LM, Pruce ML, Gabris BE, et al. Gene-targeted mice with the human troponin T R141W mutation develop dilated cardiomyopathy with calcium desensitization. *PLoS One*. 2016;11:e0167681. doi: 10.1371/journal.pone.0167681
31. Hayakawa T, Kunihiro T, Ando T, Kobayashi S, Matsui E, Yada H, Kanda Y, Kurokawa J, Furukawa T. Image-based evaluation of contraction-relaxation kinetics of human-induced pluripotent stem cell-derived cardiomyocytes: correlation and complementarity with extracellular electrophysiology. *J Mol Cell Cardiol*. 2014;77:178–191. doi: 10.1016/j.jmcc.2014.09.010
32. Sugiyama A, Hagiwara-Nagasawa M, Kambayashi R, Goto A, Chiba K, Naito AT, Kanda Y, Matsumoto A, Izumi-Nakaseko H. Analysis of electro-mechanical relationship in human iPS cell-derived cardiomyocytes sheets under proarrhythmic condition assessed by simultaneous field potential and motion vector recordings. *J Pharmacol Sci*. 2019;140:317–320. doi: 10.1016/j.jphs.2019.07.006
33. Koenig AL, Shchukina I, Amrute J, Andhey PS, Zaitsev K, Lai L, Bajpai G, Bredemeyer A, Smith G, Jones C, et al. Single-cell transcriptomics reveals cell-type-specific diversification in human heart failure. *Nat Cardiovasc Res*. 2022;1:263–280. doi: 10.1038/s44161-022-00028-6
34. Chen X, Song E. Turning foes to friends: targeting cancer-associated fibroblasts. *Nat Rev Drug Discov*. 2019;18:99–115. doi: 10.1038/s41573-018-0004-1
35. Zheng A, Chen Q, Zhang L. The Hippo-YAP pathway in various cardiovascular diseases: focusing on the inflammatory response. *Front Immunol*. 2022;13:971416. doi: 10.3389/fimmu.2022.971416
36. Xiao Y, Hill MC, Li L, Deshmukh V, Martin TJ, Wang J, Martin JF. Hippo pathway deletion in adult resting cardiac fibroblasts initiates a cell state transition with spontaneous and self-sustaining fibrosis. *Genes Dev*. 2019;33:1491–1505. doi: 10.1101/gad.329763.119
37. Mia MM, Cibi DM, Ghani SABA, Singh A, Tee N, Sivakumar V, Bogireddi H, Cook SA, Mao J, Singh MK. Loss of Yap/Taz in cardiac fibroblasts attenuates adverse remodelling and improves cardiac function. *Cardiovasc Res*. 2022;118:1785–1804. doi: 10.1093/cvr/cvab205
38. Dobaczewski M, Chen W, Frangogiannis NG. Transforming growth factor (TGF)- β signaling in cardiac remodeling. *J Mol Cell Cardiol*. 2011;51:600–606. doi: 10.1016/j.jmcc.2010.10.033
39. Liguori TTA, Liguori GR, Moreira LFP, Harmsen MC. Fibroblast growth factor-2, but not the adipose tissue-derived stromal cells secretome, inhibits TGF-beta1-induced differentiation of human cardiac fibroblasts into myofibroblasts. *Sci Rep*. 2018;8:16633. doi: 10.1038/s41598-018-34747-3
40. Schwanekamp JA, Lorts A, Sargent MA, York AJ, Grimes KM, Fischesser DM, Gokey JJ, Whitsett JA, Conway SJ, Molkentin JD. TGFBI functions similar to periostin but is uniquely dispensable during cardiac injury. *PLoS One*. 2017;12:e0181945. doi: 10.1371/journal.pone.0181945
41. Talior-Volodarsky I, Connelly KA, Arora PD, Gullberg D, McCulloch CA. Alpha11 integrin stimulates myofibroblast differentiation in diabetic cardiomyopathy. *Cardiovasc Res*. 2012;96:265–275. doi: 10.1093/cvr/cvs259
42. Gonzalez Rodriguez A, Schroeder ME, Walker CJ, Anseth KS. FGF-2 inhibits contractile properties of valvular interstitial cell myofibroblasts encapsulated in 3D MMP-degradable hydrogels. *APL Bioeng*. 2018;2:046104. doi: 10.1063/1.5042430
43. LaRocca TJ, Altman P, Jarrah AA, Gordon R, Wang E, Hadri L, Burke MW, Haddad GE, Hajjar RJ, Tarzami ST. CXCR4 cardiac specific knockout mice develop a progressive cardiomyopathy. *Int J Mol Sci*. 2019;20:2267. doi: 10.3390/ijms20092267
44. Lijnen P, Petrov V. Transforming growth factor-beta 1-induced collagen production in cultures of cardiac fibroblasts is the result of the appearance of myofibroblasts. *Methods Find Exp Clin Pharmacol*. 2002;24:333–344. doi: 10.1358/mf.2002.24.6.693065
45. Santiago JJ, Dangerfield AL, Rattan SG, Bathe KL, Cunningham RH, Raizman JE, Bedosky KM, Freed DH, Kardami E, Dixon IMC. Cardiac fibroblast to myofibroblast differentiation in vivo and in vitro: expression of focal adhesion components in neonatal and adult rat ventricular myofibroblasts. *Dev Dyn*. 2010;239:1573–1584. doi: 10.1002/dvdy.22280
46. Swaney JS, Roth DM, Olson ER, Naugle JE, Meszaros JG, Insel PA. Inhibition of cardiac myofibroblast formation and collagen synthesis by activation and overexpression of adenylyl cyclase. *Proc Natl Acad Sci USA*. 2005;102:437–442. doi: 10.1073/pnas.0408704102
47. Civitarese RA, Kapus A, McCulloch CA, Connelly KA. Role of integrins in mediating cardiac fibroblast-cardiomyocyte cross talk: a dynamic relationship in cardiac biology and pathophysiology. *Basic Res Cardiol*. 2017;112:6. doi: 10.1007/s00395-016-0598-6
48. Kudo-Sakamoto Y, Akazawa H, Ito K, Takano J, Yano M, Yabumoto C, Naito AT, Oka T, Lee JK, Sakata Y, et al. Calpain-dependent cleavage of N-cadherin is involved in the progression of post-myocardial infarction remodeling. *J Biol Chem*. 2014;289:19408–19419. doi: 10.1074/jbc.M114.567206
49. Frangogiannis NG. The extracellular matrix in ischemic and non-ischemic heart failure. *Circ Res*. 2019;125:117–146. doi: 10.1161/CIRCRESAHA.119.311148

Supplemental Material

Table S1. Primer sequences

	Forward	Reverse
<i>Gapdh</i>	5'-GGTGGGCACAGACACGAATAT-3'	5'-TCCTGGAAGATGGTGATGGGTTC-3'
<i>Nppa</i>	5'-CCTCGGAGCCTGCGAAGGTCA-3'	5'-TGTGACACACCGCAAGGGCTTG-3'
<i>Nppb</i>	5'-GACGGGCTGAGGTTGTTTA-3'	5'-ACTGTGGCAAGTTGTGCTG-3'
<i>Myh7</i>	5'-GGGTATCCGCATCTGTAGGA-3'	5'-TTGGTGTGGCCAAACTTGTA-3'
<i>Gja1</i>	5'-CTCAACAACCTGGCTGCGAAA-3'	5'-GGTGGGCACAGACACGAATAT-3'
<i>Atp2a2</i>	5'-ATTGACATCCATCAAGTCTACAACCTG-3'	5'-ATCTCAGTATTGACTCCAGTCGCC-3'
<i>Pln</i>	5'-AACTAAACAGTCTGCATTGTGACGA-3'	5'-GCCGAGCGAGTAAGGTATTGGA-3'
<i>Myh6</i>	5'-GCTTTGGGAAGTTCATCAG-3'	5'-GCCTTTAGCTGGAAGATCAC-3'
<i>Myl2</i>	5'-TTCTCAACGCCTTCAAGGTG-3'	5'-CTGGTCGATCTCTTCTTG -3'
<i>Actc1</i>	5'-AAAGCACGCCTACAGATCCC-3'	5'-TCTGAGCCTCGTCACCTACA-3'
<i>Tnnt2</i>	5'-GCCAGAGATGCTGAAGATGGT-3'	5'-GCACCAAGTTGGGCATGAAG-3'

Figure S1.

Cluster	adj.Pval	nGenes	Pathways
A	3.3e-17	63	Circulatory system development
	4.2e-16	104	Anatomical structure morphogenesis
	8.0e-15	87	Tissue development
	1.4e-13	132	Cell differentiation
	1.4e-13	119	Animal organ development
	1.4e-13	136	Cellular developmental process
	1.5e-13	26	Cardiac muscle tissue development
	2.0e-13	29	Striated muscle cell differentiation
	4.7e-13	42	Muscle structure development
	1.9e-12	31	Muscle cell differentiation
	8.3e-12	37	Circulatory system process
	1.7e-11	105	Regulation of multicellular organismal process
	2.2e-11	36	Blood circulation
	1.2e-10	30	Muscle tissue development
	2.0e-10	62	Cell adhesion
B	1.4e-19	118	Response to external stimulus
	1.4e-19	139	Regulation of multicellular organismal process
	3.9e-19	71	Tube development
	1.5e-17	119	Anatomical structure morphogenesis
	3.6e-17	55	Vasculature development
	2.3e-15	65	Circulatory system development
	2.6e-15	51	Blood vessel development
	4.0e-15	57	Tube morphogenesis
	1.2e-14	77	Cell migration
	3.1e-14	88	Locomotion
	3.1e-14	46	Blood vessel morphogenesis
	2.4e-13	79	Cell motility
	1.1e-12	40	Angiogenesis
C	6.1e-08	18	Urogenital system development
	6.1e-08	17	Renal system development
	1.1e-07	50	Anatomical structure morphogenesis
	1.6e-07	26	Tube morphogenesis
	5.5e-07	28	Tube development
	7.2e-07	22	Blood vessel development
	7.2e-07	33	Cell migration
	7.2e-07	38	Locomotion
	7.2e-07	18	Extracellular structure organization
	7.2e-07	35	Cell motility
	7.2e-07	55	Cellular response to chemical stimulus
	1.0e-06	11	Nephron development

Figure S1. Enriched pathways by K-means of each cluster revealed by gene ontogeny-term analyses.

Figure S2.

Cluster	adj.Pval	nGenes	Pathways
A	1.3e-03	9	Dilated cardiomyopathy (DCM)
	3.0e-03	8	Hypertrophic cardiomyopathy (HCM)
	3.0e-03	8	Protein digestion and absorption
	3.6e-03	7	Arrhythmogenic right ventricular cardiomyopathy (ARVC)
	6.6e-03	7	ECM-receptor interaction
B	4.2e-06	24	PI3K-Akt signaling pathway
	1.1e-05	11	Complement and coagulation cascades
	1.2e-05	11	ECM-receptor interaction
	4.5e-05	27	Pathways in cancer
	2.1e-04	18	MAPK signaling pathway
	3.1e-04	19	Neuroactive ligand-receptor interaction
	7.0e-04	8	Renin secretion
	1.3e-03	13	Focal adhesion
	2.4e-03	12	Calcium signaling pathway
	2.4e-03	12	Transcriptional misregulation in cancer
	2.5e-03	11	CGMP-PKG signaling pathway
	2.5e-03	8	Rheumatoid arthritis
	3.3e-03	15	Cytokine-cytokine receptor interaction
	3.9e-03	12	Rap1 signaling pathway
	9.9e-03	12	Ras signaling pathway
C	1.8e-03	6	Hypertrophic cardiomyopathy (HCM)
	2.3e-03	7	Cell adhesion molecules (CAMs)
	2.3e-03	10	Neuroactive ligand-receptor interaction
	2.3e-03	5	Arrhythmogenic right ventricular cardiomyopathy (ARVC)
	2.8e-03	9	Cytokine-cytokine receptor interaction
	3.4e-03	5	Rheumatoid arthritis
	3.4e-03	6	Fluid shear stress and atherosclerosis

Figure S2. Enriched pathways by K-means of each cluster revealed by Kyoto Encyclopedia of Genes and Genomes (KEGG) analyses.

Figure S3. (continued)

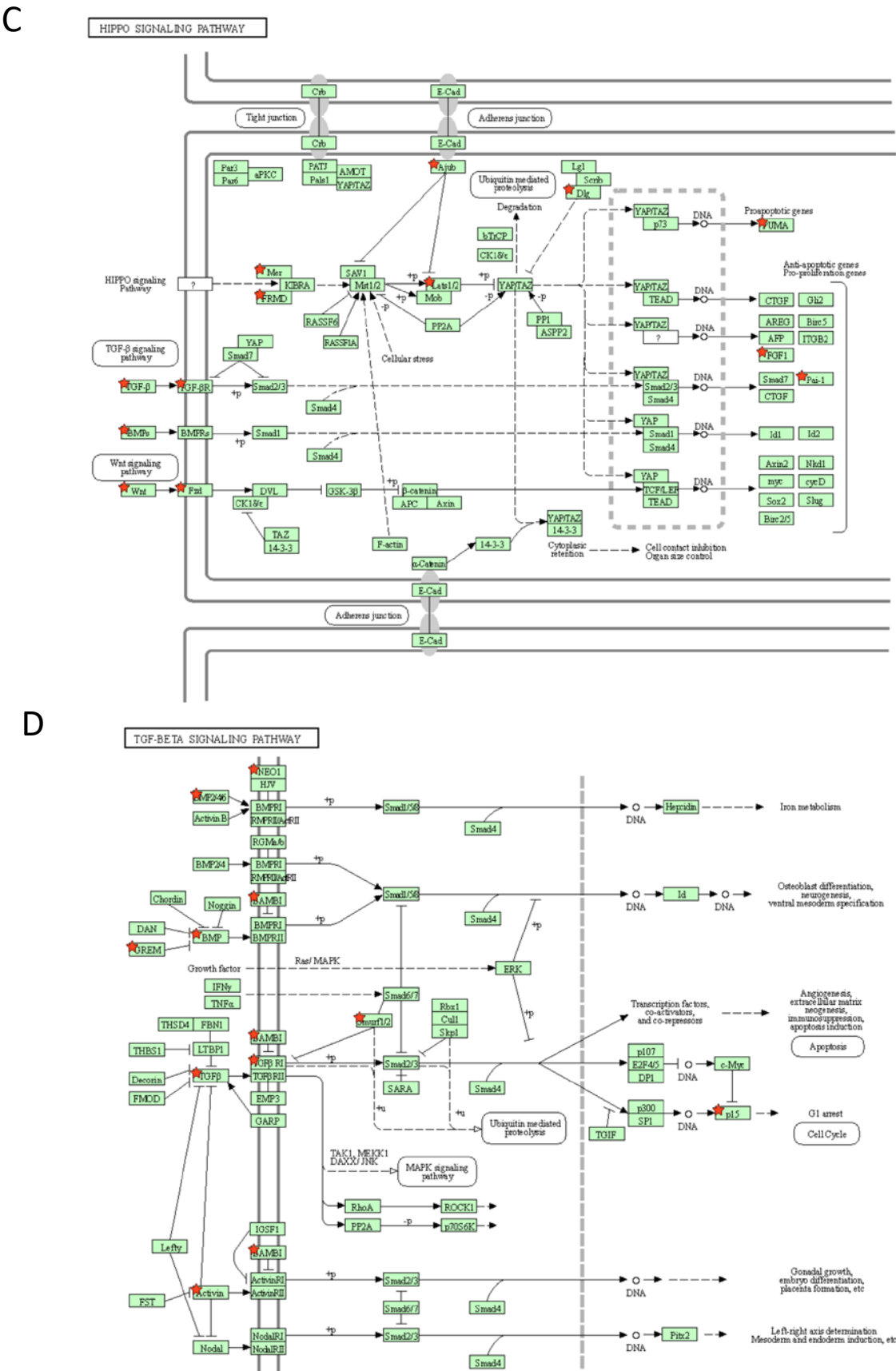


Figure S3. Pathway analyses of cardiac fibroblasts (CFs) derived from patients with dilated cardiomyopathy (DCM). (A) Extracellular matrix-associated pathways. (B) Focal adhesion signaling associated pathways. (C) Hippo signaling pathways. (D) Transforming growth factor (TGF)-beta signaling pathways. The red stars indicate the genes whose expression levels are significantly changed in DCM-CFs compared with healthy CFs.

Figure S4.

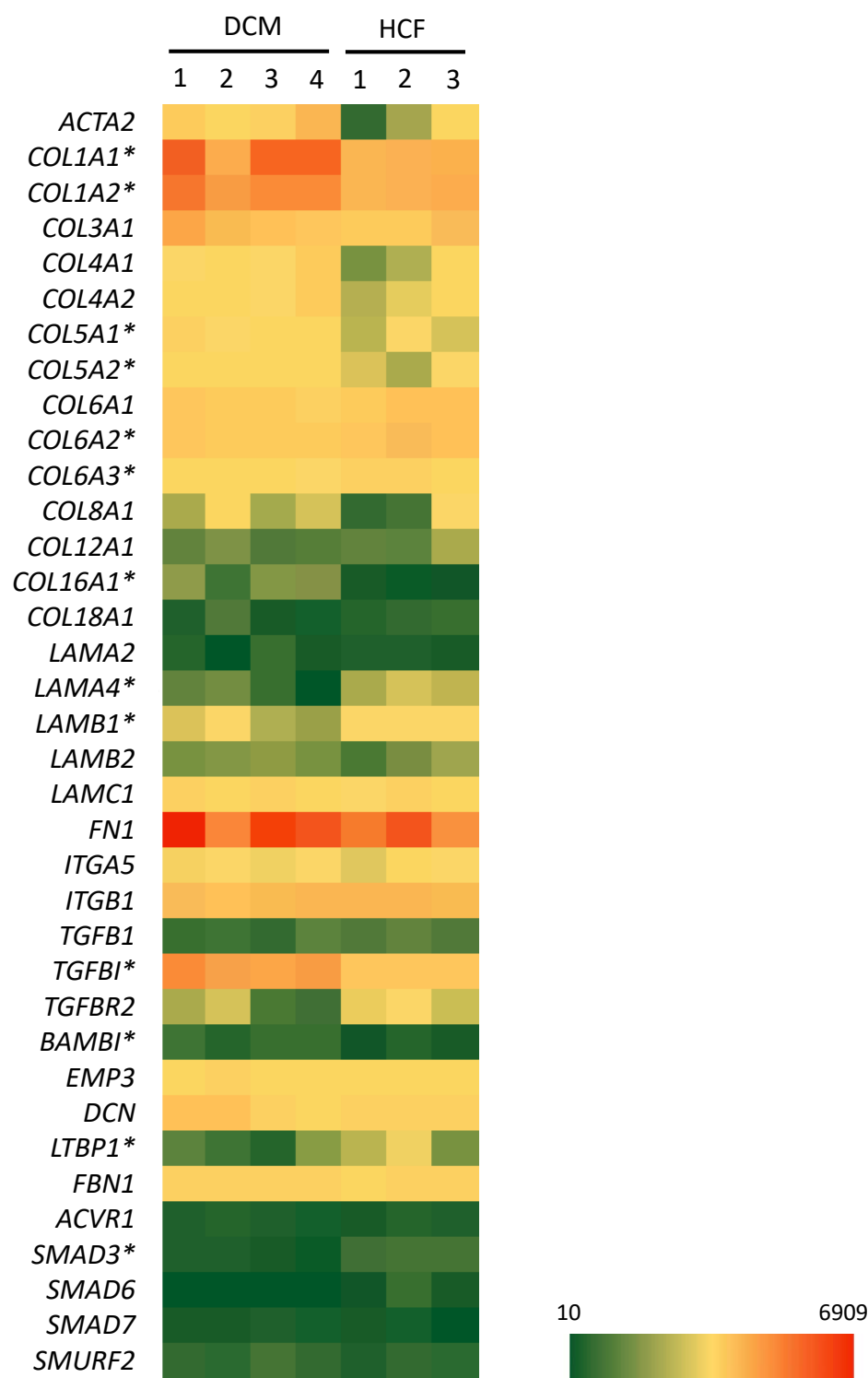


Figure S4. Expression panels of collagen-, laminin-, fibronectin-, and transforming growth factor-beta-associated genes in dilated cardiomyopathy (DCM)-cardiac fibroblasts (CFs) and healthy cardiac fibroblasts (HCFs). Transcripts per million of each gene are visualized by color scale bars. * $P < 0.05$ (DCM-CFs vs. HCFs)

Figure S5.

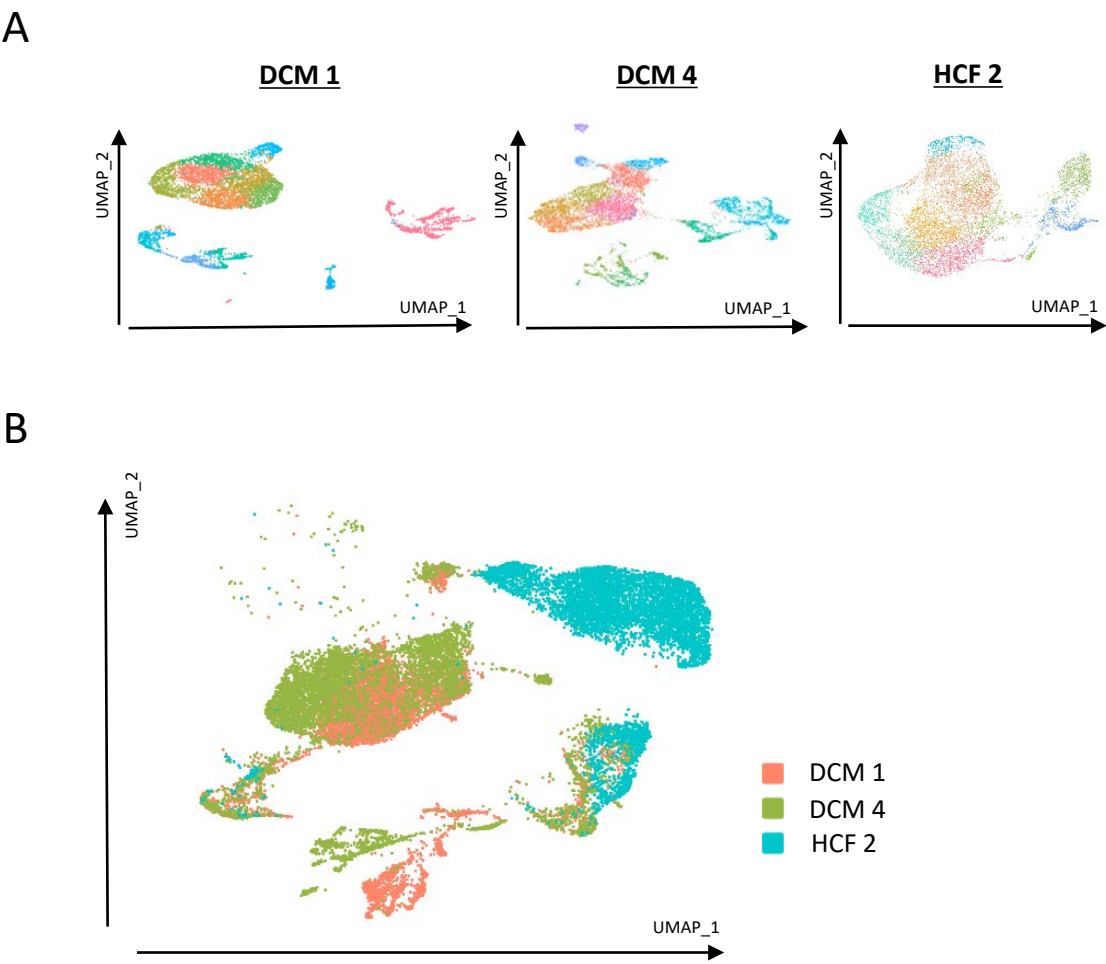


Figure S5. Single-cell RNA-sequencing for cardiac fibroblasts (CFs) derived from patients with dilated cardiomyopathy (DCM) and a healthy control (HCF). (A) Unsupervised uniform manifold approximation and projection (UMAP) analysis. DCM_1, DCM_4, and HCF_2 showed 10, 12, and 14 distinctive clusters, respectively. (B) Integrated UMAP analysis shows DCM_1 and DCM_4 demonstrating similar expression profiles compared with HCF_2.